Original Article

Thermography mapping patterns in temporal lobe epilepsy surgery

Enrique de Font-Réaulx[1], Javier Terrazo Lluch[2], Ramón López López[3], Paul Shkurovich Bialik[4], Miguel Ángel Collado Corona[4], Luis Guillermo Díaz López[5], Emilio Arch Tirado[6], Ernesto Ramírez Navarrete[7], Adalberto González Astiazarán[7]

Departments of [1]Neurosurgery, [2]Neurosurgery, [4]Neurophysiology and [7]Pediatric Neurology, Epilepsy Clinic, ABC Medical Center, [6]Neurological Center, ABC Medical Center, Mexico, Cuidad de Mexico, [3]Department of Neurorsurgery, La Raza UMAE, Social Security Mexican Institute, [5]Department of Neuroanesthesiology, National Institute of Neurology and Neurorurgery, Mexico City, Mexico.

E-mail: *Enrique de Font-Réaulx - defontreaulx@hotmail.com; Javier Terrazo Lluch - jaterrazo@hotmail.com; Ramón López López - dr_ramonzl@hotmail.com; Paul Shkurovich Bialik - paul.shkurovich@gmail.com; Miguel Ángel Collado Corona - drmcollado@hotmail.com; Luis Guillermo Díaz López - luis_diazl@hotmail.com; Emilio Arch Tirado - arch.tirado@gmail.com; Ernesto Ramírez Navarrete - soluss13@gmail.com; Adalberto González Astiazarán - neuropediatriayaprendizaje@gmail.com

*Corresponding author:
Enrique de Font-Réaulx,
Neurosurgeron, Epilepsy Clinic,
ABC Medical Center, Mexico
City, Mexico.

defontreaulx@hotmail.com

ABSTRACT

Background: In several epilepsy etiologies, the macroscopic appearance of the epileptogenic tissue is identical to the normal, which makes it hard to balance between how much cytoreduction or disconnection and brain tissue preservation must be done. A strategy to tackle this situation is by evaluating brain metabolism during surgery using infrared thermography mapping (IrTM).

Methods: In 12 epilepsy surgery cases that involved the temporal lobe, we correlated the IrTM, electrocorticography, and neuropathology results.

Results: Irritative zones (IZ) had a lower temperature in comparison to the surrounding cortex with normal electric activity (difference in temperature (ΔT) from 1.2 to 7.1, mean 3.40°C standard deviation ± 1.61). The coldest zones correlated exactly with IZ in 9/10 cortical dysplasia (CD) cases. In case 3, the coldest area was at 1 cm away from the IZ. In 10/10 dysplasia cases (cases 1–4, 6–11), there was a radial heating pattern originating from the coldest cortical point. In 2/2 neoplasia cases, the temporal lobe cortical temperature was more homogeneous than in the CD cases, with no radial heating pattern, and there were no IZ detected. In case 8, we found the coldest IrTM recording in the hippocampus, which correlated to the maximal irritative activity recorded by strip electrodes. The ΔT is inversely proportional to epilepsy chronicity.

Conclusion: IrTM could be useful in detecting hypothermic IZ in CD cases. As the ΔT is inversely proportional to epilepsy chronicity, this variable could affect the metabolic thermic patterns of the human brain.

Keywords: Cortical dysplasia, Electrocorticography, Epilepsy surgery, Functional mapping, Hypothermic irritative zone, Infrared thermography brain mapping, Refractory epilepsy, Thermography patterns

INTRODUCTION

The success of epilepsy surgery depends on removing, inhibiting, or disconnecting as much as possible the epileptogenic circuit in a safe manner. However, the question arises whether these benefits of a more extensive cytoreduction or disconnection are counterbalanced by more neurologic deficits. In this frequent scenario, the epilepsy neurosurgeon must decide whether

brain areas, specifically those located adjacent to the eloquent areas, should be affected by surgery or not. It is even harder to decide if the normal brain tissue appearance is identical to the epileptogenic tissue as it occurs in most of nonlesional cases.

Emerging novel adjuvant technology allows more extensive, safe, and effective epilepsy surgeries, as compared to incomplete resections responsible for epilepsy surgery failure. Nevertheless, it is mandatory to have an accurate, safe, noninvasive, and real-time method to differentiate between normal and epileptogenic brain tissue, as electrocorticography (ECoG) and visual inspection does not always guarantee the detection of the epileptogenic critical mass during surgery to obtain a seizure-free outcome. In other fields of neurosurgery, the use of intraoperative magnetic resonance imaging (MRI), ultrasound, neuronavigation or the use of fluorescent dyes allows more radical and safe surgeries. In epilepsy surgery, these technologies are almost useless, except in lesional epilepsy. This argument justifies the evaluation of an additional safe and in the real-time method that could be useful during epilepsy surgery as is the infrared thermography mapping (IrTM).

IrT can be used as a noncontact, noninvasive, low-cost, and real-time diagnostic tool, used to measure brain temperature. IrT has been used to detect lower or higher physiological activity.[9,10] It measures the electromagnetic radiation emitted by the objects and creates a thermal map with different color-patterns, according to the recording.[15] This technology was first used for military applications in the 1960s and since then, it has been used for medical applications in different animal species and for several purposes,[10] being one of its first medical applications in the detection of breast cancer.[5,6]

The human brain has an elevated metabolic rate with high glucose and oxygen consumption and blood flow, resulting in high heat production. There are thermic fluctuations in several physiological processes (action and resting potentials, synapsis, neurotransmission, and among others) and different thermic responses to pathologic conditions as tumors, cortical malformations, infections, and others.[12,16]

To develop a standardized and reliable lrTM procedure certain variables that can affect temperature have to be taken into consideration, such as evaporation and the variations in thermal conductivity and emissivity of different tissues.[15] The best way of reducing the impact of these variables is for the thermography record to be taken as close to the tissue as possible.

IrT has been used for detection of infections, inflammation,[10] tumors,[5,9,12] vascular diseases,[2] trauma, burns,[11] multiple sclerosis, epilepsy,[7,14] headache, and neurodegenerative diseases with different results[16] and questionable methodology. High-grade gliomas have a lower temperature than the surrounding normal brain because of a lower metabolic rate related to edema and necrosis.[9] There are publications with a series of different neoplastic surgical cases, where IrT has been used to plan the resection margins in real-time during surgery. IrT could be used by the neurosurgeon, as a tool to obtain an anatomic physiological and physiopathological map in real-time to guide brain lesions resections[2] and for functional mapping.

The propagation of thermal waves during a seizure with increased local temperature has been described since the neural hyperexcitation may increase cortical perfusion and thereby generate thermal changes,[16] but the accuracy of these data is questionable. Although there are few studies in humans, it is known that there is a relationship between brain temperature, cerebral blood flow (CBF), focal brain activity, and the functional state of the neurons in epilepsy.[16] As already shown in some studies in animals, the temperature of the epileptogenic zone varies if the IrT is performed during the interictal or ictal period since the CBF will be different if the epileptogenic focus is active during measurement or not. In a cortical dysplasia (CD) zone, the metabolism will be decreased to a greater or lesser extent according to the type of dysplasia, but the core of this lesion is hypometabolic with a lower perfusion rate.[3,13,17] The application of IrTM for surveillance in vascular neurosurgery for aneurysm clipping has been recently published by our group[1] and has been proposed as a method for the registration and fusion of preoperative 3D MRI with intraoperative 2D IrT.[4]

MATERIALS AND METHODS

Methods and technique description

Underbalanced general anesthesia using bispectral index-monitoring system, we carried out conventional fronto-parieto-temporal craniotomy in each case. Before the dura mater incision, we recorded its temperature using a laser infrared pointer thermometer (Floureon©). Immediately after the dura incision, using a handheld thermal imaging camera (Kmoon©) that combines the pictures taken with surface temperature measurement, which provides real-time thermal imaging, we performed a basal IrTM of the brain surface exposed, taking the recordings as close as possible to the brain to obtain the best accuracy. The infrared thermal camera can turn the thermal irradiation of the brain surface exposed to a visible image. It quickly evaluates the different thermal gradients of the brain, and it can also blend the visible and infrared images. We placed the electrodes grid for the initial ECoG [Figure 1a]. Perforated grids with coordinates were placed in the IrTM under the ECoG grids, obtaining a precise concordance of each grid perforation with the ECoG electrodes [Figure 1a and b]. Before IrTM, we recorded the depth of anesthesia, hemoglobin, hematocrit, and CO_2 were measured by arterial gasometry, and the body

temperature was recorded using an esophageal thermometer. There were an ambient temperature and relative humidity in the operating room. Then, we gently removed the ECoG grid, leaving the IrTM grid with coordinates in place over the brain surface and pictures were taken [Figure 1b]. We correlated the coordinates of the IrTM perforated grid with respect to their corresponding electrode of the ECoG grid. We performed a second IrTM with the laser pointer infrared thermometer and recorded the cortical temperature of each grid perforation coordinate.

Statistical analysis

Demographic data were compared using Fisher's exact test for categorical variables and Student's *t*-test for continuous variables. The bivariate or multivariate correlations were analyzed with the Pearson, Spearman, and Mann–Whitney U-tests. The *P* significance threshold was set at <0.05.

Ethical considerations

This study was submitted and approved by the Research Committee and Bioethics Committee of our institution. All participants or tutors signed the informed consent form and patient registration was han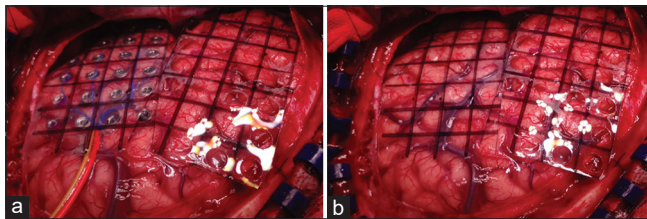dled with strict confidentiality, in accordance with the ethical principles for medical research on human subjects of the Declaration of Fortaleza, Brazil, in 2013.

RESULTS

We included 12 patients, 3 males and (25%) and 9 females (75%); the age range was 11–66 years with an average of 32.5 years. The value of the asymmetry index was 0.795, with a Kurtosis of 0.047. The average and standard deviation of the temperatures recorded in irritative zones (IZ) and the maximal brain temperatures are almost equal, so the existing sample size is valid for this study [Table 1]. All patients were right-handed.

Cases 5 and 12 were reported with neoplastic etiologies: low-grade astrocytoma and dysembryoplastic neuroepithelial tumor (DNET), respectively. In case 5, the astrocytoma did not involve the temporal, frontal, or parietal surface and a biopsy by craniotomy was performed [Table 2].

The humidity in the operating room remained fixed at 40% in all surgeries. The temperature range in the operating room at the beginning of the surgery was 17–20°C (mean of 18.85°C) and the final range of 18–21°C (mean of 19.1°C). The esophageal temperatures at the beginning of the surgery were between 33.7 and 36.5°C with an average of 34.93°C, being the final esophageal temperatures of 33.6–36.6°C with a mean of 35.4°C. The patients stayed within stable physiological hemodynamic parameters during the surgical procedure to maintain cerebral self-regulation. The temperature recordings range is shown in Table 3.

In 2/2 neoplasia cases (cases 5 and 12), the temporal lobe cortical temperature was more homogeneous than in the rest of the cases, with no radial heating pattern, and there were no IZ detected using ECoG. In the rest of the cases, we identified IZ, which had lower temperature recordings by IrTM in comparison to the surrounding cortex with normal electric activity (difference in temperature [ΔT] from 1.2 to 7.1, mean 3.40°C standard deviation ± 1.61). The coldest IrTM zones correlated exactly with IZ in 9/10 CD cases (cases 1, 2,

Figure 1: (a) Infrared thermography grid placed over the electrocorticography (ECoG) grid in the left temporal lobe and infrared thermography grid placement in the frontal lobe. Note that, the infrared thermography grid has the same size as the electrocorticography grid designed to have a very precise anatomical correlation. (b) The final position of both infrared thermography mapping grids in left frontal and temporal lobes, after removing the ECoG grid.

	n	Range	Minimum	Maximum	Mean	Standard error	Standard deviation	Variance	Skewness	Kurtosis
Table 1: Descriptive statistics.										
Age	12	55	11	66	32.5	4.8092	16.6596	277.545	0.795	0.047
Duration Epi	12	43	2	45	15	3.616	12.5263	156.909	1.423	1.997
Age of onset	12	63.9	0.1	64	17.5083	4.7986	16.6228	276.319	2.193	5.908
Meningeal temp	12	10.2	27.7	37.9	34.1916	0.8066	2.7942	7.808	−1.228	1.682
Irritative zone temp	12	6.4	28.5	34.9	30.5333	0.5346	1.8519	3.43	1.241	1.469
Maximal brain temp	12	4.9	31.7	36.6	33.9416	0.503	1.7427	3.037	0.259	−1.198
Delta T	12	5.9	1.2	7.1	3.4083	0.4673	1.6188	2.621	0.958	1.205

The mean and standard deviation of the irritative zone temperature and m aximal brain temperature tend to be equal

Table 2: Clinical case description.

Case	Gender/age in years	Epilepsy onset in years	Radiologic diagnosis	Surgery
1	Female/22	7	LMTLS	Left FTL+AH
2	Female/13	8	Left focal cortical insular dysplasia	Left insular ápex resection
3	Male/47	20	RMTLS	Right FTL+AH
4	Female/38	31	LMTLS	Left FTL+AH
5	Male/66	2	Left temporal-insular low-grade glioma	Tumor biopsy by craniotomy
6	Male/22	9	LMTLS	Left FTL+AH
7	Female/26	2	LMTLS	Left FTL+AH
8	Female/11	11	Left hemimegalencephalia	Left functional hemispherectomy
9	Female/29	19	RMTLS	Right FTL+AH
10	Female/32	10	RMTLS	Right FTL+AH
11	Female/56	45	LMTLS	Left FTL+AH
12	Female	16	DNET	Left FTL+AH

LMTLS: Left mesial temporal lobe sclerosis, consider dual temporal pathology; RMTLS: Right mesial temporal lobe sclerosis, consider dual temporal pathology; FTL+AH: Functional temporal lobectomy+Amygdalo–hippocampectomy

4, and 6–11), excluding the III-B and DNET cases. In case 3, the coldest IrTM point was at 1 cm of distance from the IZ. In 10/10 CD cases (1–4, 6–11), there was a radial heating pattern originating from the hypothermic IZ (HIZ) and the hottest point was the most distant from the HIZ. In case 8, we found the coldest IrTM recording in the hippocampus which correlated to the maximal irritative activity recorded by strip electrodes [Table 3]. All HIZ were resected. Neuropathology diagnosis is shown in Table 4.

Clinical cases and IrTM results

The meningeal temperature range was 27.7–37.9°C (mean 34.19°C, DS ± 2.79). The IZ temperature was 28.5–34.9°C (mean 30.53°C DS ± 1.85). The maximum temperature recorded was 31.7–36.6°C (mean 33.94°C DS ± 1.74). The IrTM using the pointer thermometer technique and acetate grid are shown in Figure 2. The infrared thermal panoramic pictures are shown in Figure 3.

The averages of the recorded temperatures were compared, and a significant difference was found between IZ temperature and maximal brain temperature (0.0001), as well as between meningeal temperature and IZ temperature (0.004) [Graph 1a]. When constructing the scatter plot, a correlation was observed (being higher in the range of 30–40°) between the variables so that the Pearson correlation coefficient was calculated between these two variables (r = 0.596). When the temperature in IZ is increased, it is also increased the maximal brain temperature [Graph 1b]. It draws attention that in addition to the correlation between these variables, the difference between their means is highly significant.

A trivariable plot was built to analyze the behavior between age, meningeal temperature, and age of onset, where two trends are observed based on this analysis. When the age increases in the 13–28 years interval, the meningeal temperature is higher,

Table 3: Temperature recordings range by infrared thermography mapping.

Case	Meningeal temperature	Maximal IZ temperature recorded	Maximal brain temperature recorded	ΔT
1	33.1	29.3	32	2.7
2	30.5	30.1	33.6	3.5
3	35.2	31.6	33.8	2.2
4	27.7	30.6	33.4	2.8
5	34.3	32	35.3	3.3
6	37.9	29.1	31.7	2.6
7	33.9	34.9	36.1	1.2
8	36.6	29	33.5	4.5
9	36.2	32.2	36.6	4.4
10	35.7	29.1	36.2	7.1
11	35.5	30.0	31.7	1.7
12	33.7	28.5	33.4	4.9

IZ: Irritative zone, ΔT: Difference in temperature. All measurements are in °C

Table 4: Neuropathology diagnosis according to the international league against epilepsy classification.

Case	Neuropathology diagnosis
1	III-A
2	II-A
3	III-A
4	III-A
5	III-B (diffuse astrocytoma "Wild Type" OMS Grade II, IDH1m negative, Ki67 positive 15%, and p53 positive <5%)
6	III-A
7	III-A
8	III-D
9	III-A
10	III-A
11	III-A
12	DNET

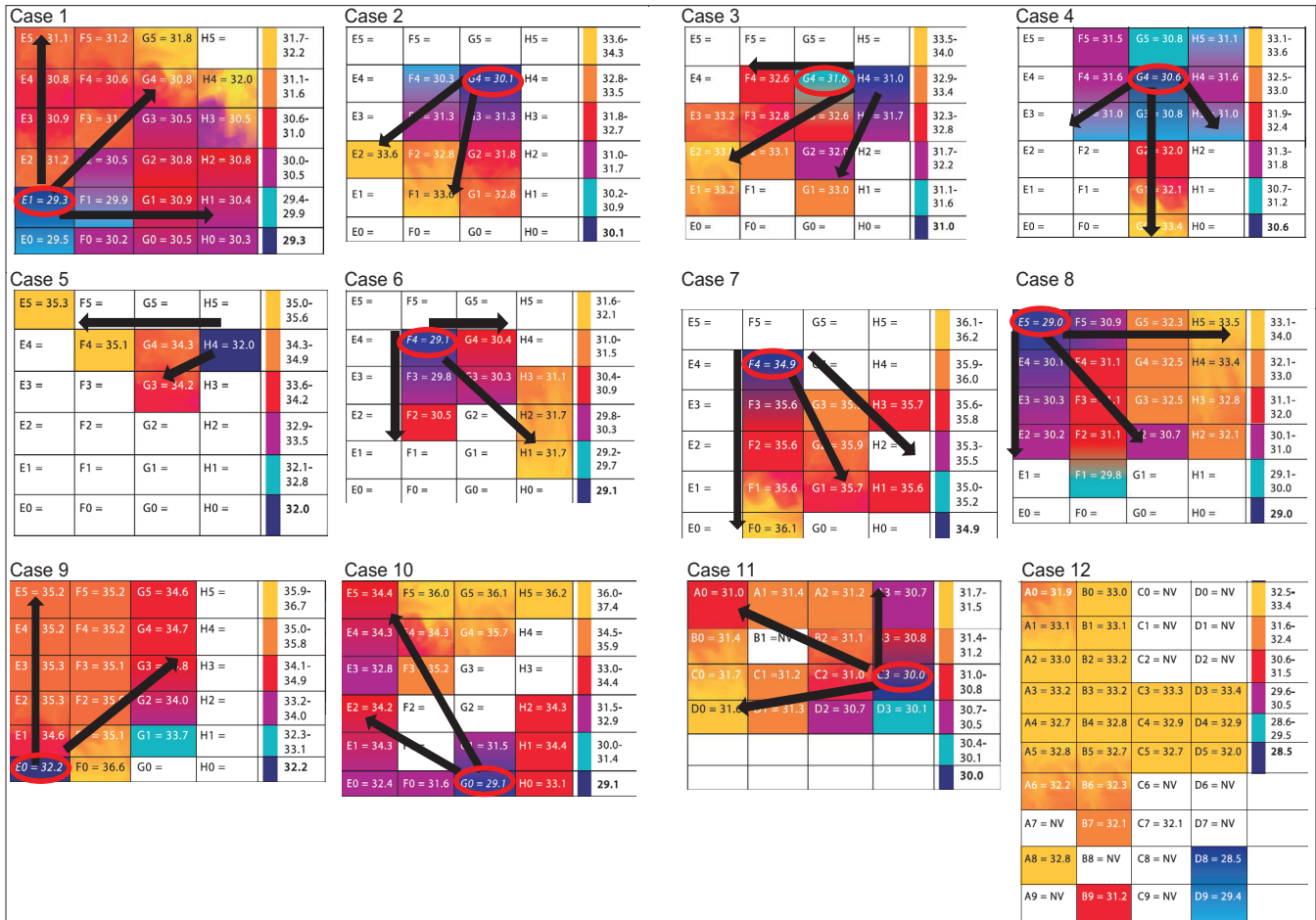DNET: Dysembryoplastic neuroepithelial tumor

Figure 2: Cases numbers and graphic representation of the temperature lectures as recorded in °C. The infrared thermography mapping grid lectures show a color representation using the thermographic palette, where deep blue represents the lowest and yellow the highest temperature. Note the radial heating pattern indicated with black arrows where the coldest temperature lecture is in the hypothermic irritative zones (HIZ) in 90% or at 1 cm of distance to the HIZ in 10% of the dysplasia cases. The temperature in italics surrounded by a red oval corresponds to the IZ detected by electrocorticography.

and in the range of 22–56 years, when increasing the age, the meningeal temperature is decreased [Graph 2a]. A trivariable plot was built between age, age of onset, and ΔT to evaluate the behavior between these three variables. It was observed that by increasing the epilepsy chronicity, the value of ΔT decreases. Furthermore, interestingly, the age of onset does not influence this trend [Graph 2b].

To assess the behavior of all temperatures recorded by age and subject, a box plot was made to compare the medians based on the second and third quartile, where it is observed that in the range of 26–56 years old, the value of the medians decreases with respect to age [Graph 3].

DISCUSSION

An ideal trans operatory functional imaging adjuvant device must allow the obtaining of real-time information, be secure and offer high sensitivity and specificity to ensure the detection of metabolism differences, guide the resection of epileptogenic tissue, and the prevention of normal cortex resection.

Thermography-based blood flow imaging has been widely investigated in cardiovascular procedures, establishing a quantitative correlation between blood flow and temperature (r = 0.96). Watson observed that changes in blood temperature are related to changes in brain blood flow, whereas cortical brain temperature is determined by CBF-metabolism coupling, and the infrared image could be sufficiently sensitive to detect ischemia.[6,7] Arterial blood and core temperatures are higher than the exposed surface of the brain since they descend by evaporation and exposure to the environment. Therefore, local microvascular blood flow self-regulation of the brain can be used as a natural reference for monitoring thermal variability and changes with IrT imaging of the cerebral cortex during surgery. It has been described
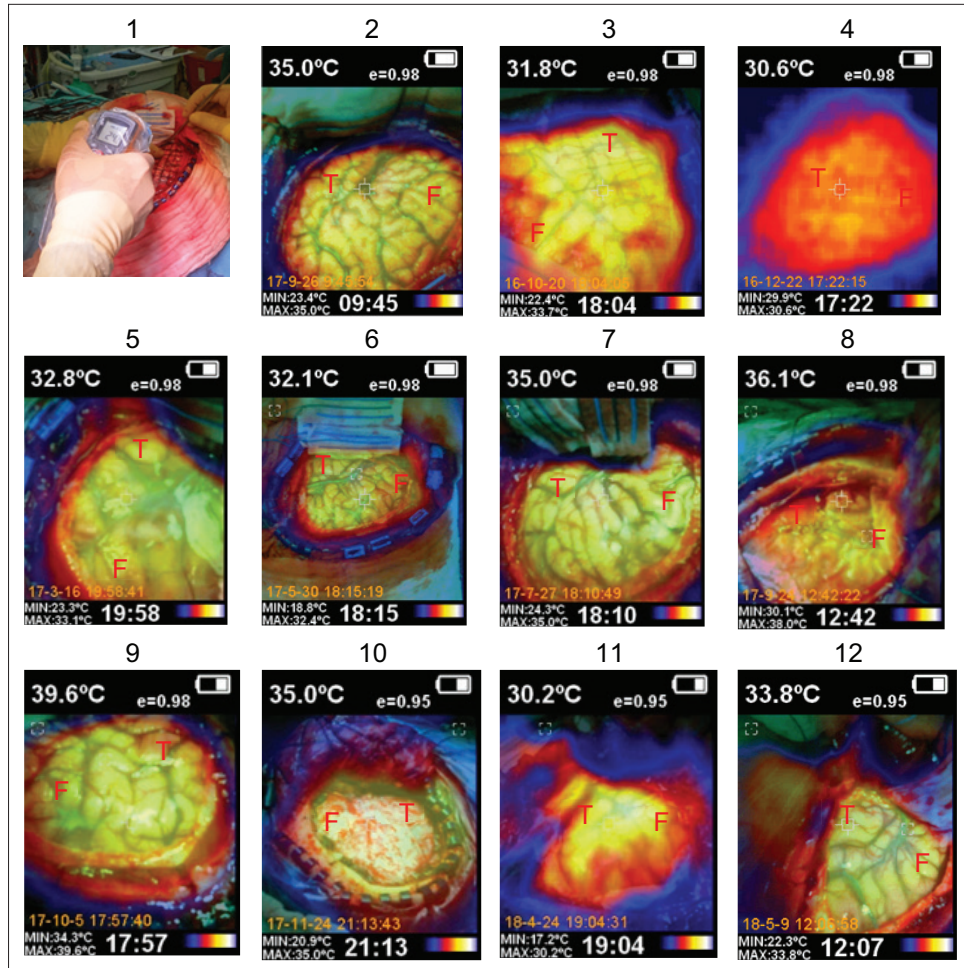
Figure 3: Picture numbers correspond to case numbers. The red letter F is placed over the frontal lobe and T over the temporal pole. The values are similar to the temperature recorded using the infrared thermographic laser pointer thermometer.

as an immediate and significant temperature decrease in the artery distal to the occlusion and the tissue perfused by it.[7,16]

The use of IrT in neurosurgery began in 2001 in patients with the painful complex syndrome.[5] New generations of infrared cameras are equipped with a system of high resolution to a minimum temperature difference. These images can show small changes in surface temperature related to both local and systemic physiological processes. Intraoperatory surveillance using thermography in neurosurgery has been described in the resection of tumors and in the monitoring of patency of bypass in arteriovenous malformations, in which it demonstrated adequate correlation compared with such conventional methods as CT, postoperative magnetic resonance, Doppler, and angiography, among other methods.

The advantages of cortical IrTM in neurosurgery are as follows: it is noninvasive, safe, provides real-time imaging, is fast and accurate, and does not require the use of any contrast media or dyes. It has broad potential applications in neurosurgery for the measurement of cerebral metabolism (tumors, vascular

pathology, epilepsy, brain abscesses, trauma, and spine, among others). It allows for analysis of comparative physiology, has potential applications for research, measures thermogenesis, and is useful for analyzing metabolic consumption. Moreover, it is low-cost, useful for analyzing cooling by evaporation and diffusion of heat; each case has its own control, as often there is a healthy brain exposed in craniotomy. The disadvantages are that its use is not yet standardized and it only measures the temperature of the exposed surface. As with any imaging study subject to estimate that requires analytical modeling done by the software included in the equipment data processor, the reading can be affected by ambient temperature and environmental humidity.

In these cases, we described epilepsy surgery neuropathology diagnosis correlated to ECoG and IrTM recordings results. For this purpose, we monitored the cortical temperature in critical moments during surgery, where the epileptogenic neocortical tissue had to be removed and the normal cerebral tissue preserved.
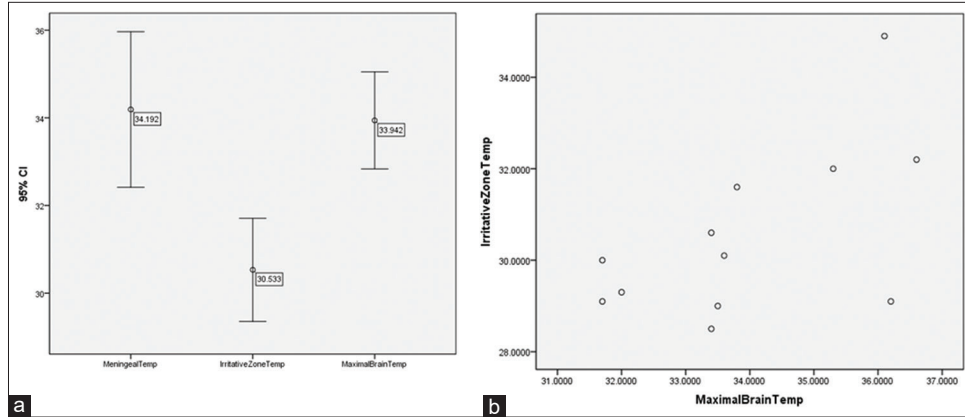
Graph 1: (a) Error graphs of registered temperatures. Averages and dispersions are observed where values with the lowest recorded temperatures were in irritative zones (IZ). (b) Dispersion between the IZ temperature and the maximal brain temperature. It is observed that by increasing the temperature in the IZ, the maximal brain temperature is also increased.
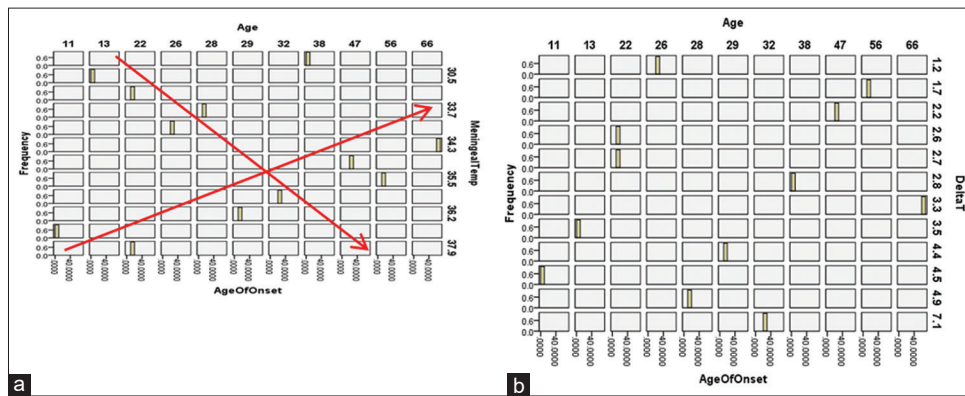
Graph 2: (a) Trivariable histogram between age, age of onset, and meningeal temperature: it is observed that at an older age, the temperature tends to stabilize. (b) Trivariate analysis between age, start age, and ΔT: it is observed that at the increase of the epilepsy chronicity, it decreases the value of ΔT.
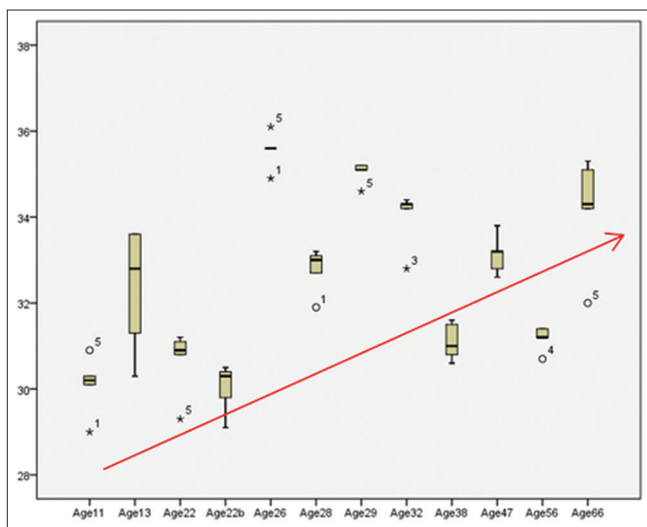
Graph 3: The median difference between registered temperatures. It is observed that from the age of 26 to 56 years old, the medians of the recorded temperatures decrease.

Using IrTM, we found a ΔT of up to 7.1°C between the IZ detected by ECoG and a clear radial heating pattern around the HIZ [Table 3 and Figure 3]. Neuropathology demonstrated several CD types according to the International League against Epilepsy (ILAE) classification [Table 4] in the cortex resected, where the lowest temperature also corresponded to the IZ. This allows us to assume that important differences in the cerebral metabolism between the normal and the dysplastic cortex could be detected by IrTM.

In 9/10 (90%) of our dysplasia cases (excluding type III-B and DNET), the IZ correlated with the coldest temperature recorded by IrTM, except for case 3, where the IZ was at 1 cm from the coldest region detected by IrTM. In case 5, there were no epileptiform discharges detected by ECoG, but there was a ΔT of 3.3°C, between the lowest and the highest tissue temperature, that could be explained by the abnormal metabolic demands related to the neoplastic versus the normal tissue.

After the visual analysis of the color charts where the temperatures obtained by IrTM of the IZ and temperatures

of the surrounding tissue were recorded, we can concluded that it is evident the temperature decreases in the IZ, even though it was the first temperature obtained from the surgical field this was the coldest temperature in most of the cases, compared to both tumor cases (cases 5 and 12), where temperatures are similar and no heating pattern was observed. The zones of the brain with higher temperatures could be the euthermic normometabolic areas and the zones where recorded lower temperatures could correspond to the region where the metabolic function of the brain tissue is dysfunctional.

The positive correlation between the longer time since epilepsy onset and the higher difference between the coldest cortical temperature and the IZ, the observation that the ΔT is inversely proportional to epilepsy chronicity, as well as the observation that the temperature in the IZ is increased, it also increases the maximal brain temperature, opens a new discussion about the metabolic cellular changes related to epileptogenic mechanisms, which goes beyond the scope of this research. Nevertheless, it is consistent with the assumption that CD may not be static abnormalities.[8] Furthermore, the positive correlation between the meningeal temperature and the temperature of the IZ detected by ECoG, indicates the degree of relationship between these two variables and the importance of this data.

The observation that from the age of 26–56 years old, the medians of the recorded temperatures decrease are of uncertain significance in the context of epilepsy. Nevertheless, brain metabolism and therefore, temperature could be affected by the myelinization process and circulatory variables in the younger, and by circulatory variables and demyelinization process in older persons, altogether with lifestyle and comorbidity associated with age.

CONCLUSION

The IrTM is a real-time, noninvasive method that requires no manipulation of tissue or the use of contrast dyes or filters. It is safe, efficient, and low-cost, hence it is a promising adjuvant for intraoperative monitoring in epilepsy surgery. The areas identified with CD, with active epileptogenic activity detected by ECoG, were colder than the dysplastic nonirritative tissue and the normal cortex by this method. According to this data, we found that in CD, the HIZ has a ΔT of up to 7.1°C with respect to the normal and the dysplastic nonepileptogenic brain tissue. In case 1, the cortical hypothermia correlated to the hypometabolic zone is detected by single emission computed tomography and positron emission tomography (PET).

Given the results of these consecutive cases, we consider that IrTM could be a useful method to improve surgical outcomes, avoiding resecting normal cortex, or leaving epileptogenic dysplastic tissue. More cases are required to determine the potential use of IrT in neurosurgery in general for metabolic mapping and in epilepsy surgery in particular.

We found that the decrease of the temperature measured by IrTM of the HIZ corresponds to the actual gold standard that is the ECoG to identify the IZ in epilepsy surgery and that the resected tissue corresponded with CD Type II-A, III-A, according to the ILAE classification. The IZ was the coldest IrTM lecture point. A radial heating pattern was evident starting from this point in all the CD cases, excluding 2 cases diagnosed as III-B and III-D (DNET).

The ΔT is inversely proportional to epilepsy chronicity in the CD, the longer time since epilepsy onset there is a higher difference b etween the c oldest cortical t emperature and the IZ, and when the temperature in the IZ is increased, it also increases the maximal brain temperature, supports the previous concept that CD is not static lesions[8] and could affect wide neural circuits during life.

One limitation of our study is the sample size, but despite this, it was possible to obtain significant differences an d positive correlation of the results. According to our findings, where the IZ are the coldest brain regions measured by IrTM, we can hypothesize that IZ is hypometabolic as it has been previously demonstrated by PET studies. The brain metabolism intraoperative information provided by the IrTM could be essential during epilepsy surgery, to guide the surgical progress and to identify changes and abnormalities of cerebral metabolism in real-time, which can be correlated to ECoG.

We consider that the IrTM can be an additional method for trans-operatory monitoring of brain metabolism based on lower temperature correlated with the epileptogenic activity. It could be used to identify areas of different temperature gradients in real-time, guiding the resection and preserving normal tissue, to achieve better results in terms of seizure control and safety in epilepsy surgery.

Declaration of patient consent

The authors certify that they have obtained all appropriate patient consent.

Financial support and sponsorship

Nil.

Conflicts of interest

There are no conflicts of interest.

REFERENCES

1. de Font-Réaulx Rojas E, Martínez Ochoa EE, López López R, López Díaz LG. Infrared thermography brain mapping surveillance in vascular neurosurgery for anterior communicating artery aneurysm clipping. Surg Neurol Int 2018;9:188.
2. Ecker RD, Goerss SJ, Meyer FB, Cohen-Gadol AA, Britton JW, Levine JA. Vision of the future: Initial experience with intraoperative real-time high-resolution dynamic infrared imaging. Technical note. J Neurosurg 2002;97:1460-71.
3. Elkins KC, Moncayo VM, Kim H, Olson LD. Utility of gray-matter segmentation of ictal-interictal perfusion SPECT and interictal 18F-FDG-PET in medically refractory epilepsy. Epilepsy Res 2017;130:93-100.
4. Hoffmann N, Weidner F, Urban P, Meyer T, Schnabel C, Radev Y, *et al*. Framework for 2D-3D image fusion of infrared thermography with preoperative MRI. Biomed Tech (Berl) 2017;62:599-607.
5. Kateb B, Yamamoto V, Yu C, Grundfest W, Gruen JP. Infrared thermal imaging: A review of the literature and case report. Neuroimage 2009;47 Suppl 2:T154-62.
6. Kerr J, Zealand N. Review of the effectiveness of infrared thermal imaging (thermography) for population screening and diagnostic testing for breast cancer. Rev Lit Arts Am 2004;3:1-49.
7. King HH, Cayce CT, Herrin J. Thermography examination of abdominal area skin temperatures in individuals with and without focal-onset epilepsy. Explore (NY) 2017;13:46-52.
8. Najm IM, Tilelli CQ, Oghlakian R. Pathophysiological mechanisms of focal cortical dysplasia: A critical review of human tissue studies and animal models. Epilepsia 2007;48 Suppl 2:21-32.
9. Naydenov E, Minkin K, Penkov M, Nachev S, Stummer W. Infrared thermography in surgery of newly diagnosed glioblastoma multiforme: A technical case report. Case Rep Oncol 2017;10:350-5.
10. Salles MS, da Silva SC, Salles FA, Roma LC Jr., El Faro L, Bustos Mac Lean PA, *et al*. Mapping the body surface temperature of cattle by infrared thermography. J Therm Biol 2016;62:63-9.
11. Saxena AK, Willital GH. Infrared thermography: Experience from a decade of pediatric imaging. Eur J Pediatr 2008;167:757-64.
12. Steiner G, Sobottka SB, Koch E, Schackert G, Kirsch M. Intraoperative imaging of cortical cerebral perfusion by time-resolved thermography and multivariate data analysis. J Biomed Opt 2011;16:016001.
13. Suárez-Piñera M, Mestre-Frusco A, Ley M, González S, Medrano S, Principe A, *et al*. SPECT de perfusión, SISCOM y PET 18F-FDG en la valoración del paciente epiléptico fármaco-resistente candidato a cirugía de epilepsia. Rev Esp Med Nucl Imagen Mol 2015;34:350-7.
14. Sunderam S, Osorio I. Mesial temporal lobe seizures may activate thermoregulatory mechanisms in humans: An infrared study of facial temperature. Epilepsy Behav 2003;4:399-406.
15. Tattersall GJ. Infrared thermography: A non-invasive window into thermal physiology. Comp Biochem Physiol A Mol Integr Physiol 2016;202:78-98.
16. Wang H, Wang B, Normoyle KP, Jackson K, Spitler K, Sharrock MF, *et al*. Brain temperature and its fundamental properties: A review for clinical neuroscientists. Front Neurosci 2014;8:307.
17. Wintermark P, Lechpammer M, Warfield SK, Kosaras B, Takeoka M, Poduri A, *et al*. Perfusion imaging of focal cortical dysplasia using arterial spin labeling: Correlation with histopathological vascular density. J Child Neurol 2013;28:1474-82.